

# Acoustic interactions between inversion symmetric and asymmetric two-level systems

A. Churkin<sup>1,2</sup>, D. Barash<sup>2</sup>, and M. Schechter<sup>1,\*</sup>

<sup>1</sup> *Department of Physics, Ben Gurion University of the Negev, Beer Sheva 84105, Israel and*

<sup>2</sup> *Department of Computer Science, Ben Gurion University of the Negev, Beer Sheva 84105, Israel*  
(Dated: today)

Amorphous solids, as well as many other disordered materials, display remarkable universality in their low temperature acoustic properties. This universality is attributed to the attenuation of phonons by tunneling two-level systems (TLSs), facilitated by the interaction of the TLSs with the phonon field. Recently a Two-TLS model was introduced, where it was shown that inversion symmetric TLSs, i.e. TLSs having their two states related by local inversion symmetry, dictate phonon attenuation at low temperatures, and are responsible for the universal phenomena. The Two-TLS model suggests resolution to some long standing questions regarding the universal phenomena, such as the smallness and universality of the tunneling strength, and the energy scale of 3K below which universality is observed. A crucial part of the Two-TLS model lies in the magnitude and spatial dependence of effective TLS-TLS interactions involving inversion symmetric TLSs. Here we calculate numerically, using conjugate gradients method, the effective elastic TLS-TLS interactions for inversion symmetric and asymmetric TLSs, for pure and disordered solids, in two and three dimensions. We verify analytical estimates used in the Two-TLS model. We further show that the disorder induced power reduction of the spatial dependence of the interaction persists to short distances, not much larger than the interatomic distance. Our results provide strong support to the Two-TLS model, and contribute to the better understanding of the microscopic structure of amorphous solids and the low temperature properties of glasses.

## I. INTRODUCTION

The existence of two-level tunneling defects as a generic property in amorphous systems was postulated four decades ago[1, 2] in an attempt to explain the remarkable universality in the low energy characteristics of amorphous solids as were found earlier by Zeller and Pohl[3]. In what is now known as the Standard Tunneling Model (STM)[1, 2, 4] the interaction of the tunneling two-level systems (TLSs) with the phonon field is given by

$$H_{\text{TLS-ph}} = \sum_j \sum_{\alpha, \beta} \gamma_{js}^{\alpha\beta} S_j^z \frac{\partial u_j^\alpha}{\partial \mathbf{r}_j^\beta}. \quad (1)$$

Here  $S_j^z = \pm 1/2$  denote the two states of the TLS at site  $j$ ,  $u^{\alpha\beta} \equiv \partial u^\alpha / \partial \mathbf{r}^\beta$  is the phonon field, where  $u$  is the phonon amplitude,  $\alpha, \beta \equiv x, y, z$ , and  $\gamma$  is the TLS-phonon interaction parameter. The interaction of the phonon field with the tunneling amplitude of the TLS is small, and therefore neglected[1, 2].

The TLS-phonon interaction as given in Eq.(1) gives rise to an effective TLS-TLS interaction mediated by the phonon field[5, 6], which takes the form

$$H_{\text{TLS}}^{\text{eff}} = \sum_{ij} U_{ij} S_i^z S_j^z \quad (2)$$

where  $U_{ij}$  is effectively random interaction with  $1/r^3$  dependence for distance  $r \gg a_0$ . Here  $a_0$  denotes the typical interatomic distance. The STM, however, assumes that the TLSs are non-interacting, an assumption that is sufficient to explain many of the properties of amorphous

solids in the universal regime,  $T < T_U \approx 3\text{K}$  (notable exceptions are the phenomena of spectral diffusion[5] and the dipole gap arising at very low temperatures,  $T < 0.1\text{K}$ [7-9]). Reconciliation of the assumption of non-interacting TLSs with the presence of TLS-phonon interaction is explained by the low density of TLSs, and consequent smallness of the typical interaction.

Recently a new model was suggested, which is based on the different properties of the interaction of inversion symmetric and inversion asymmetric TLSs with the phonon field[10]. A TLS in which the two states are related to each other by inversion with respect to a mid-point, e.g. 180° flip of CN impurity in a KBr lattice, does not interact with the phonon field, but only with the second derivative of the phonon amplitude[6]

$$H_{\text{TLS-ph}}^{\text{sym}} = \sum_j \sum_{\alpha, \beta, \delta} \zeta_{\alpha\beta\delta}(\mathbf{r}_j) \frac{\partial^2 u_j^\alpha}{\partial \mathbf{r}_j^\beta \partial \mathbf{r}_j^\delta} \tau_j^z, \quad (3)$$

where we denote by  $\tau$  the symmetric TLSs, to differ from the asymmetric TLSs denoted by  $S$ . This form of the interaction leads, in three dimensions, to a long distance dependence of  $1/r^4$  and  $1/r^5$  for the acoustic mediated  $S$  TLS- $\tau$  TLS ( $S$ - $\tau$ ) effective interactions and  $\tau$  TLS- $\tau$  TLS ( $\tau$ - $\tau$ ) effective interactions respectively[6]. In two dimensions similar analysis to the one carried in Ref. [6] leads to  $1/r^2, 1/r^3, 1/r^4$  spatial dependence of the  $S$  TLS- $S$  TLS ( $S$ - $S$ ),  $S$ - $\tau$ , and  $\tau$ - $\tau$  interactions respectively.

Where the above is correct for 2 impurities in an otherwise pure lattice, the presence of disorder introduces deviations from inversion symmetry, and a finite, albeit small interaction between a  $\tau$ -TLS and the phonon field. In Ref.[10] it was argued that for systems with strong disorder the TLS-phonon interaction can be written as

$$H_{\text{TLS-ph}}^{\text{tot}} = \sum_{j,\alpha,\beta} \gamma_s^{\alpha\beta}(\mathbf{r}_j) S_j^z u_j^{\alpha\beta} + \sum_{j',\alpha,\beta} \gamma_w^{\alpha\beta}(\mathbf{r}_{j'}) \tau_{j'}^z u_{j'}^{\alpha\beta}. \quad (4)$$

The small dimensionless parameter of the theory[10] is defined by  $g \equiv \gamma_w/\gamma_s$ . This parameter is proportional to the deviations from inversion symmetry, and therefore to the ratio between the strain and interatomic lattice spacing, i.e. in strongly disordered systems  $g \approx 0.01 - 0.03$ . The resulting effective elastic TLS-TLS interaction takes the form[10]

$$H_{S\tau}^{\text{eff}} = \sum_{ij} U_{ij}^{SS} S_i^z S_j^z + \sum_{ij} U_{ij}^{S\tau} S_i^z \tau_j^z + \sum_{ij} U_{ij}^{\tau\tau} \tau_i^z \tau_j^z \quad (5)$$

where in three dimensions (two dimensions) all interactions decay as  $1/r^3$  ( $1/r^2$ ) at distances  $r \gg a_0$ , and their typical values at near neighbor distance are related by

$$U_0^{\tau\tau} \approx g U_0^{S\tau} \approx g^2 U_0^{SS}. \quad (6)$$

It is further argued[10] that the above long distance power law dependence of the interaction persists down to a short distance cutoff, which is not much larger than the interatomic spacing, for lack of another relevant length scale in the system. The form of the Hamiltonian (5), (6), i.e. the strength and spatial dependence of the three TLS-TLS interactions, and its subsequent analysis have led to a significant advance in the understanding of the low temperature universality in glasses[10]. The universality and smallness of phonon attenuation[11, 12] were shown to be a consequence of the generic characteristics of the  $\tau$  TLSs, and the appearance of universality below  $T_U \approx 3\text{K}$  was attributed to the gapping of the S-TLSs below the energy scale of  $U_0^{S\tau} \approx g U_0^{SS} \approx g T_G \approx 3\text{K}$ , where  $T_G$  is the glass temperature. The enhancement of the single particle S-TLS DOS at higher temperatures results in their domination of acoustic attenuation, and the limiting of the universal characteristics of amorphous and disordered solids to  $T < T_U$ .

The Two-TLS model further derives, and quantifies, some of the central assumptions of the STM. The DOS of the relevant TLSs at low temperatures, the  $\tau$ -TLSs, is found to be finite at very low energies and rather homogeneous for energies smaller than 3K. The assumption of noninteracting TLSs is supported by the fact that at low temperatures the S-TLSs are frozen, and the typical  $\tau - \tau$  interaction  $U_0^{\tau\tau} \approx 0.1\text{K}$  is smaller by a factor of  $g$  in comparison to the typical  $\tau$ -TLS energy, which dictates the typical energy scale of the universal phenomena. Thus, within the Two-TLS model TLS-TLS interactions can be neglected except at very low temperatures. However, this possibility to neglect the interactions does not depend on the small concentration of TLSs, but on the form of the Hamiltonian (5), (6). This is in line with the existence of universal phenomena in disordered lattices such as KBr:CN, where there are strong evidences to

the notion that each CN impurity constitutes a two-level system. Thus, the TLS-DOS in disordered lattices is not small, the relevant TLSs are  $\tau$ -TLSs, between which the interaction is small and can therefore be neglected, and the smallness of the DOS of detected TLSs is related to the fact that only TLSs with appreciable tunneling amplitude can be detected. Note that in KBr:CN the TLS is formed by each CN low energy state and the state related to it by a CN flip[10, 13–15], and is thus a  $\tau$ -TLS, where all other single particle states of a given CN impurity are much higher in energy, as they constitute an S excitation with respect to the CN low energy state[10].

The Two-TLS model, and specifically the Hamiltonian (5), was derived microscopically for strongly disordered lattices. However, the strong evidence for the equivalence of the phenomenon of the low temperature universality in disordered lattices and amorphous solids (as well as other disordered systems, e.g. disordered polymers, metallic glasses, quasicrystals)[12, 16, 17], strongly suggests that the mechanism leading to universality in disordered lattices and amorphous solids is the same. Thus, validation of the Two-TLS model is significant both for the resolution of the long standing problem of universality in disordered and amorphous solids, and for the advance of our understanding of the microscopic structure of amorphous solids. The two crucial points of the Two-TLS model are the form of the Hamiltonian (5), (6), and the resulting structure of the DOS of the  $\tau$  and S TLSs. With regard to the latter, the results in Ref.[10] are supported by a comprehensive numerical calculation given in Ref.[18]. With regard to the former, a significant step was made in Ref.[15], where  $\gamma_w, \gamma_s$  were explicitly calculated for KBr:CN. The obtained ratio of  $\gamma_w/\gamma_s \approx 0.02$  and value  $\gamma_w \approx 0.1\text{eV}$  are both in agreement with theory[10] and with the experimental value for the coupling constant for the relevant TLSs at low temperatures,[19, 20]. These results support both the Two-TLS model and the notion that it is indeed CN flips that constitute the TLSs for KBr:CN. However, the ab-initio and DFT calculations[15] required the use of very small samples, not allowing the study of the effective TLS-TLS interactions and their distance dependence.

In this paper we use the conjugate gradients method to study the magnitude and spatial dependence of the elastic impurity-impurity interactions in KBr:CN. Since CN impurities possess also charge, the elastic energy is derived by calculating first the total interaction energy and subtracting from it the direct electric TLS-TLS interaction. Calculations are performed for S-S, S- $\tau$ , and  $\tau$ - $\tau$  interactions in two and three dimensions, in both pure and disordered lattices, as function of distance between the TLSs. In Sec. II we present the calculation setup. Our results are presented in Sec. III, and conclusions in Sec. IV.

$\alpha\alpha$	$A_{\alpha\alpha}$ (kJ/mol)	$a_{\alpha\alpha}$ (1/Å)	$B_{\alpha\alpha}$ (Å <sup>6</sup> kJ/mol)
KK	158100	2.985	-1464
CC	259000	3.600	-2110
NN	205020	3.600	-1803
BrBr	429600	2.985	-12410

TABLE I: Interatomic potential parameters (taken from Ref. [21]). Cross-interaction parameters were calculated from the combining rules  $A_{\alpha\beta} = (A_{\alpha\alpha}A_{\beta\beta})^{1/2}$ ,  $a_{\alpha\beta} = (a_{\alpha\alpha} + a_{\beta\beta})/2$ ,  $B_{\alpha\beta} = (B_{\alpha\alpha}B_{\beta\beta})^{1/2}$ .

## II. THE MODEL

All our calculations are carried for CN impurities in KBr lattice. For some even size  $N$ , we arrange initially  $N \times N$   $K^+$  and  $Br^-$  ions in the two dimensional grid (or  $N \times N \times N$  ions in 3D grid) having the distance  $r = 3.2735 \text{Å}$  between  $K^+$  and  $Br^-$  ions [21]. Then we replace some of the  $Br^-$  ions with  $CN^-$  ions. The  $K^+$  and  $Br^-$  ions are assumed to carry +1 and -1 charges respectively, while the charge of the  $CN^-$  ion is represented by fractional charges  $q_C = -1.28$  and  $q_N = -1.37$  placed on the carbon and nitrogen atoms, and the additional charge  $q_{center} = +1.65$  is placed at the center of mass [22]. The C-N bond length is fixed at  $1.17 \text{Å}$ , while the distances of the carbon and nitrogen atoms from the center of mass are fixed at  $0.63 \text{Å}$  and  $0.54 \text{Å}$  respectively [22]. Interatomic potential is calculated by the formula:

$$V_{\alpha\beta}(R) = A_{\alpha\beta} \exp(-a_{\alpha\beta}r) + \frac{B_{\alpha\beta}}{r^6} + K \frac{q_{\alpha}q_{\beta}}{r}. \quad (7)$$

The interatomic potential parameters  $A_{\alpha\beta}$ ,  $a_{\alpha\beta}$  and  $B_{\alpha\beta}$  are taken from Ref. [21] and shown in Table I, and  $K = 1389.35 \text{ÅkJ/mol}$ .

Non-linear conjugate gradients method (Fletcher-Reeves) is used to find the closest local minimum of the system potential energy  $U$ . Periodic boundary conditions are used to simulate the infinite crystal.

In order to study the spatial dependence of the CN-CN interactions in the KBr:CN crystal we calculate the potential energy  $U_r$  (as described above) for KBr:CN grids, containing only two CN ions. The CNs are placed at some distance  $R$  from each other in some direction  $[x, y, z]$ . For example, if the first CN ion is placed at coordinate  $[0, 0, 0]$  in the grid (3D array),  $R = 3$  and the direction is  $[2, 2, 2]$ , then the second CN is placed at  $[R \cdot x, R \cdot y, R \cdot z] = [6, 6, 6]$ . For a given distance  $R$  and direction  $[x, y, z]$  we calculate the energies for several different orientations of CN ions in the grid and we use these energies to evaluate the S-S, S- $\tau$  and  $\tau$ - $\tau$  interactions, as explained in detail below. Because the non-linear conjugate gradients method is very time consuming for large samples, we use both two dimensional and three dimensional grids. The three dimensional grids relate to the relevant experimental systems, whereas the two dimensional grids allow us

to study spatial dependence of CN-CN interactions at longer distances.

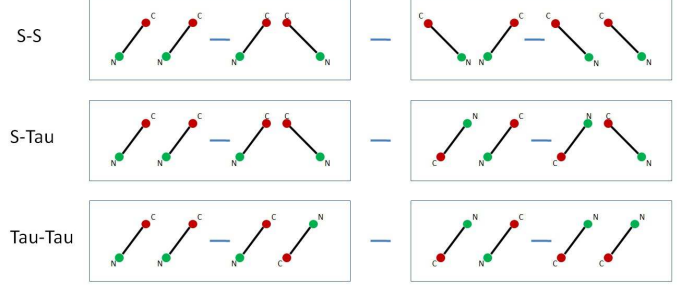


FIG. 1: S-S, S- $\tau$  and  $\tau$ - $\tau$  interactions calculation in 2D grid with two CN ions placed at some distance  $r$  from each other. Each pair of CN ions in the figure represents the energy  $U_r$  of the low energy state, where the ions are placed in the direction shown in the figure. The interaction energy  $U$  for each one of the interactions is calculated by  $U = (U_r(1) - U_r(2)) - (U_r(3) - U_r(4))$ .

We now describe the algorithm used to calculate the S-S, S- $\tau$  and  $\tau$ - $\tau$  interactions. We start by finding the low energy states for a single CN impurity in an otherwise pure KBr:CN lattice. In two dimensions these low energy states are four-fold degenerate, along the square diagonals. In three dimensions these states are eight-fold degenerate along the in-space diagonals. We emphasize that although for a single CN impurity the ground state degeneracy is lifted by tunneling, for strong disordered systems (CN concentration  $0.2 < x < 0.7$ ) the CN-CN interactions are much larger than the tunneling amplitude, and therefore it is the interaction with neighboring CN impurities that breaks the single impurity ground state degeneracy. The treatment of tunneling can then be deferred until the bias energies are determined[10]. Since in this paper we are concerned only with the energy bias of the different orientational states resulting from interactions with other CN impurities, tunneling is neglected altogether. This is also in line with our chosen calculation method, which does not allow tunneling over large barriers.

Let us now describe the calculation of the interaction, starting with two dimensions, see also Fig. 1. For the S-S interaction at some distance  $r$  we calculate first the elastic energy  $U_r^{\text{elas}}(1)$ . Both CN ions are placed initially at an angle  $\phi_{1,2} = \pi/4$  (angles are calculated between the direction of the N-C vector and the x-axis). The whole system is then relaxed. The CN-CN interaction results in a small shift in the CN positions ( $\ll a_0$ ) and angles ( $\ll \pi$ ). The resulting total energy of the system,  $U_r^{\text{tot}}(1)$  and positions of the CN molecules are recorded. The direct electric energy between the two CN molecules  $U_r^{\text{elec}}(1)$  is calculated from the relaxed positions of the CN molecules, and  $U_r^{\text{elas}}(1) = U_r^{\text{tot}}(1) - U_r^{\text{elec}}(1)$  is deduced. We then follow the same procedure to calculate  $U_r^{\text{elas}}(2)$  with first CN ion having  $\phi_1 \approx \pi/4$  and the second ion is rotated with  $\phi_2 \approx 3\pi/4$ ,  $U_r^{\text{elas}}(3)$  with first

CN ion rotated having  $\phi_1 \approx 3\pi/4$  and the second ion with  $\phi_2 \approx \pi/4$  and  $U_r^{\text{elas}}(4)$  having both CN rotated with  $\phi_{1,2} \approx 3\pi/4$ . Finally, the S-S interaction energy is calculated by:  $U^{\text{elas}}(\text{S-S}) = (U_r^{\text{elas}}(1) - U_r^{\text{elas}}(2)) - (U_r^{\text{elas}}(3) - U_r^{\text{elas}}(4))$ . S- $\tau$  and  $\tau$ - $\tau$  interactions energies are calculated in a similar way. The difference in S- $\tau$  and  $\tau$ - $\tau$  interactions calculation is that  $U_r^{\text{elas}}(3)$  and  $U_r^{\text{elas}}(4)$  are calculated while the first CN ion instead of being rotated is flipped, i.e.  $\phi_1 \approx 5\pi/4$ . Additionally, for the  $\tau$ - $\tau$  calculation the second CN in  $U_r^{\text{elas}}(2)$  and  $U_r^{\text{elas}}(4)$  is flipped:  $\phi_2 \approx 5\pi/4$ , see Fig. 1.

Interaction	Angle	$U_r1$	$U_r2$	$U_r3$	$U_r4$
S-S	$\phi_{(CN1)}$	$\pi/4$	$3\pi/4$	$\pi/4$	$3\pi/4$
	$\theta_{(CN1)}$	0.955	0.955	0.955	0.955
	$\phi_{(CN2)}$	$\pi/4$	$\pi/4$	$3\pi/4$	$3\pi/4$
	$\theta_{(CN2)}$	0.955	0.955	0.955	0.955
S- $\tau$	$\phi_{(CN1)}$	$\pi/4$	$3\pi/4$	$\pi/4$	$3\pi/4$
	$\theta_{(CN1)}$	0.955	0.955	0.955	0.955
	$\phi_{(CN2)}$	$\pi/4$	$\pi/4$	$5\pi/4$	$5\pi/4$
	$\theta_{(CN2)}$	0.955	0.955	2.186	2.186

TABLE II: Approximate values of  $\phi$  and  $\theta$  angles of two CN ions in the three dimensional grids, used in the calculation of  $U_r(i)$  for S-S and S- $\tau$  interactions.

In three dimensions the calculations are carried in a similar way. Since the low energy states of a single CN impurity are eight-fold degenerate, each CN impurity, whereas it can assume only a single flip, can rotate in six different directions. We thus specify for each calculation which of the allowed rotations is performed, see Table II.

As mentioned above, the spatial dependence of the S- $\tau$  and  $\tau$ - $\tau$  elastic interactions is modified in the presence of disorder. We therefore repeat the above calculations for CN-CN interactions in the presence of a third and fourth impurities. As the purpose of these added impurities is to introduce strain disorder, they are placed in a given position and orientation, and are then relaxed with the whole system for each configuration of the two “original” CNs between which the interaction is calculated.

No	1st CN position	2nd CN position	3rd CN position	4th CN position	$\phi$ of 3rd CN	$\phi$ of 4th CN
1	[0, 2]	$[2 \cdot r, 2]$	$[2 \cdot r + 1, 3]$		$\pi/4$	
2	[0, 2]	$[2 \cdot r, 2]$	$[2 \cdot r + 1, 5]$	$[2 \cdot r, 0]$	$3\pi/4$	$\pi/4$

TABLE III: Positions of four CN ions and the angles of third and fourth CN ions in the two dimensional grids, for direction [2, 0]. First row corresponds to the data denote “3 CNs 1” in Figs. 4, 5. Second row with the first three and with all four impurities correspond to the data denoted “3 CNs 2” and “4 CNs 2” in the above figures respectively.

Direction	1st CN position	2nd CN position	3rd CN position	$\phi$ of 3rd CN	$\theta$ of 3rd CN
[1, 1, 0]	[0, 0, 0]	$[r, r, 0]$	$[r, r, 2]$	$\pi/4$	0.955
[2, 0, 0]	[0, 0, 0]	$[2 \cdot r, 0, 0]$	$[2 \cdot r + 1, 3, 0]$	$3\pi/4$	0.955

TABLE IV: Positions of three CN ions and the angles of third CN ion in the three dimensional grids, for directions [1, 1, 0] and [2, 0, 0].

### III. RESULTS

The S-S, S- $\tau$ , and  $\tau$ - $\tau$  elastic interaction energies [ $U^{\text{elas}}(\text{S-S})$ ,  $U^{\text{elas}}(\text{S-}\tau)$  and  $U^{\text{elas}}(\tau\text{-}\tau)$ ] for two CN impurities in an otherwise pure lattice calculated for two dimensional grids of size  $50 \times 50$  are plotted in Fig. 2 and Fig. 3 for directions [2, 0] and [3, 1], respectively. The 1 unit of distance in the plot is chosen to be the distance between two closest ions in the grid, which is about  $3.2735 \text{ \AA}$ . Calculations are performed up to maximal distance of 20 ions in diagonal, as at larger distances boundary condition effects become significant. Data at the shortest distances ( $\sim a_0$ ) is disregarded, as it shows irregularity dictated by the properties of the lattice at near neighbor distance.

Since our available distance range is limited, lattice discreteness is expected to play a role. Indeed, the exact values of the magnitude of the elastic interactions at short distance and their distance dependence depends on details such as the direction between the two CN impurities, and the detailed position and orientation of the additional impurities, see below. Still, our numerical results strongly support both the typical magnitude of the various elastic interactions (S-S, S- $\tau$ ,  $\tau$ - $\tau$ ) at short distance, and their spatial dependence, as discussed above.

The magnitude of the elastic interactions we find numerically is in agreement with experiments, and with their interpretation by the Two-TLS model. The elastic S-S interaction at short distance is of the order of 100K, which is the same order of the glass temperature in KBr:CN. The elastic S- $\tau$  interaction is of the order of 3K, which is  $g$  times smaller, and is characteristic of the temperature below which universality is observed[10]. The elastic  $\tau$ - $\tau$  interaction is of the order of 0.1K (another factor of  $g$  smaller), in agreement with the theory of the Two-TLS model, and with low energy experiments reporting interaction phenomena at this energy scale[8, 9]. The spatial dependence is also in good agreement with theory[6], as the S-S, S- $\tau$ , and  $\tau$ - $\tau$  elastic interactions behave as  $1/r^\alpha$ , with  $\alpha \approx 2, 3, 4$  respectively. We note that because the magnitude of the elastic  $\tau$ - $\tau$  interactions at distances larger than a few times  $a_0$  is not much larger than our numerical error, reliable results for the  $\tau$ - $\tau$  interaction are available only for two dimensional samples in the (2,0) direction.

The power law reduction of the  $r$  dependence of the elastic S- $\tau$  interaction upon the introduction of disorder (from 4 to 3 in three dimensions, from 3 to 2 in two di-



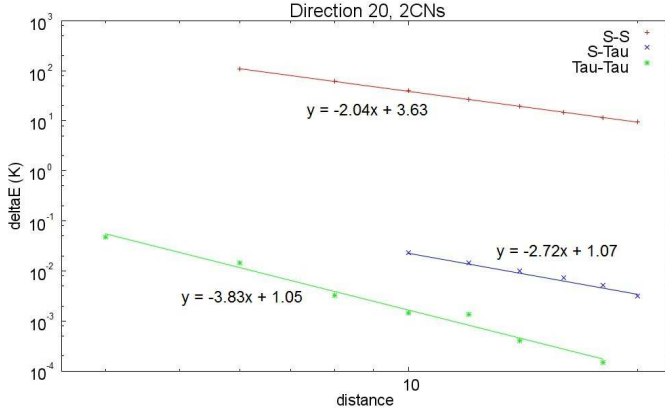


FIG. 2: Spatial dependence of the elastic S-S, S- $\tau$  and  $\tau$ - $\tau$  interactions of 2 CNs placed in the direction [2,0] in 2D grid of size 50x50. Here and in subsequent figures energies are given in Kelvin units,  $1(\text{KJ/mol})/k_B = 120.274K$ . Solid line are best linear fits, where slopes denote the power law distance dependence of the interaction.

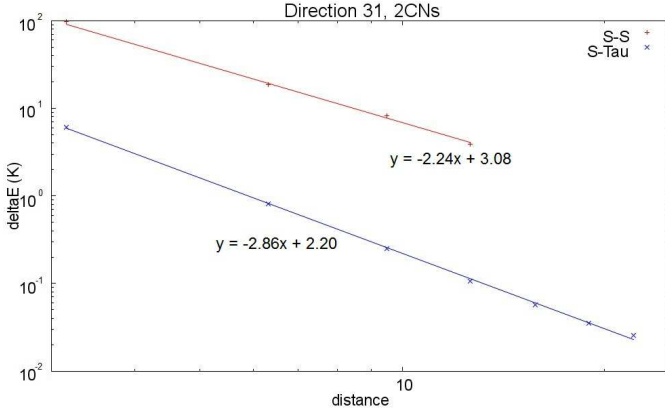


FIG. 3: Spatial dependence of the elastic S-S and S- $\tau$  interactions of 2 CNs placed in the direction [3,1] in 2D grid of size 50x50.

mensions) is a crucial aspect of the Two-TLS model[10]. In order to test this result numerically, we introduce additional, third and fourth, impurities to the sample, see Table III. We then repeat the calculations above for the original two CN impurities. The additional impurities introduce strain disorder at the location of the measured TLSs. The results for the spatial dependence of the elastic S- $\tau$  interaction with two, three and four CN impurities in 2D grid in direction [2,0] are shown in Fig. 4. Despite the large variance in the calculated power laws for the different disorder configurations, a clear reduction of the power law is obtained, consistent with the theoretically predicted reduction from 3 to 2[10]. Our results here also support the theoretical prediction that disorder does not affect the typical magnitude of the elastic S- $\tau$  interaction at short distance. In Fig. 5 the overall results of S-S, S- $\tau$  and  $\tau$ - $\tau$  elastic interactions in the 2D grids are plotted.

The factor of  $g \approx 0.03$  separating the magnitudes of the S-S, S- $\tau$ , and  $\tau$ - $\tau$  interaction, the insignificance of disorder for the typical magnitude of these interactions at the shortest distances, and at the same time the effect of disorder on the spatial dependence of the S- $\tau$  interactions, are all clearly demonstrated. A central result of this paper is the finding that the power law dependence of the various interactions, and specifically the disordered induced spatial dependence of the S- $\tau$  interactions ( $\sim 1/r^2$  in two dimensions,  $\sim 1/r^3$  in three dimensions, see below), persists to very short distances, not much larger than the interatomic spacing.

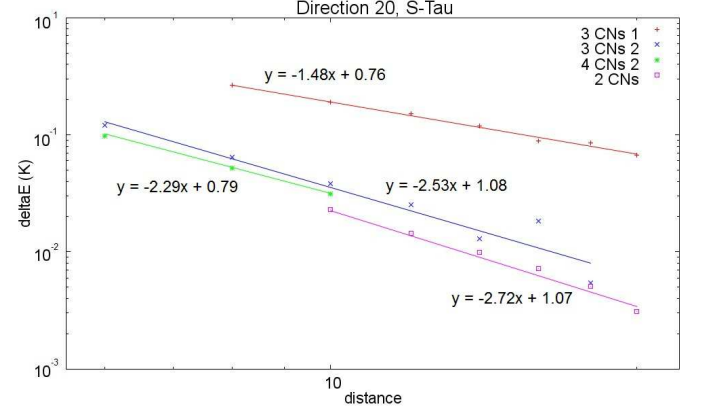


FIG. 4: Spatial dependence of the elastic S- $\tau$  interaction with two, three and four CNs placed in the direction [2,0] in 2D grid of size 50x50. Data for 2 CNs corresponds to S- $\tau$  interaction in a pure KBr lattice. Data for 3 and 4 CNs corresponds to S- $\tau$  interaction (calculated for impurities 1 and 2) in a disordered lattice (introduced by impurities 3 and 4). Positions and orientations of third and fourth impurities are given in Table III. In Table III row 1 corresponds to the data denoted here “3 CNs 1” and row 2 to the data in “3 CNs 2” and “4 CNs 2”.

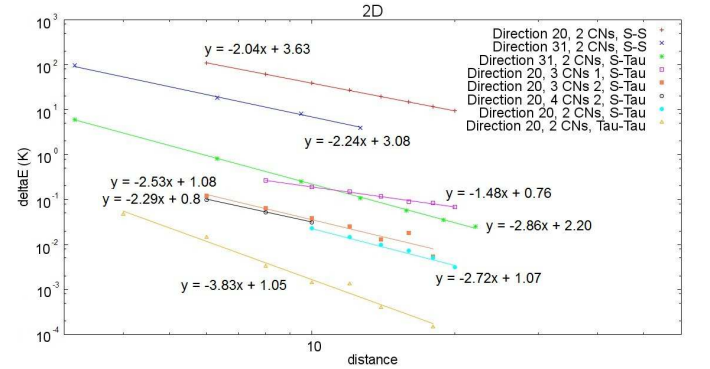


FIG. 5: Spatial dependence of the elastic S-S, S- $\tau$  and  $\tau$ - $\tau$  interactions in 2D grids of size 50x50.

Similar calculation, for the elastic S-S interaction in a pure lattice, and for the elastic S- $\tau$  interactions in a pure lattice and with disorder strain induced by a third

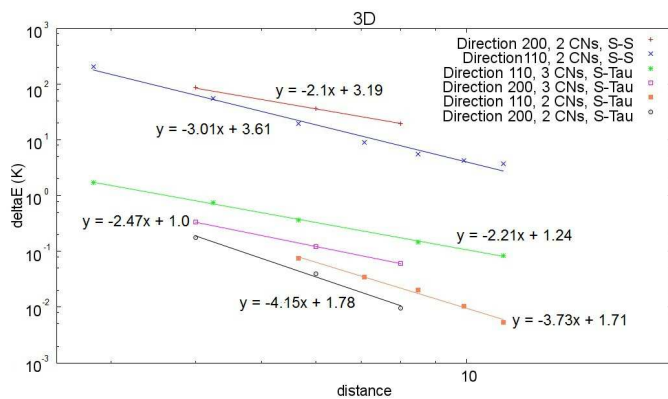


FIG. 6: Spatial dependence of the elastic S-S and S- $\tau$  interactions in 3D grids of size 20x20x20. Positions and orientations of impurities are given in Table IV

impurity, were performed for three dimensional samples of size 20x20x20. Results for directions [1,1,0] and [2,0,0] with impurities in the positions specified in Table IV are shown in Fig. 6. For the elastic S- $\tau$  interaction in an otherwise pure lattice we find for the spatial dependence a good agreement with the  $1/r^4$  behavior predicted by theory. For the power law of the spatial dependence of both the elastic S-S interaction and the elastic S- $\tau$  interaction with strain disorder we obtain values of 2.1 – 3.01. We attribute this large variance in exponents to the significance of lattice discreteness and boundary conditions, consequences of the small lattice size. Still, the reduction of the exponent of the spatial dependence of the elastic S- $\tau$  interaction upon the introduction of disorder is clearly shown. With regard to the typical magnitude of the interactions, our results clearly reproduce the correct magnitude of order 100K for the elastic S-S interaction at short distances, and the much smaller, by factor of

$g \approx 0.03$ , magnitude of the elastic S- $\tau$  interaction, with and without disorder.

#### IV. CONCLUSIONS

Using conjugate gradients method we have calculated the elastic interactions between rotations and flips of CN impurities in a KBr lattice. CN flips constitute two states related to each other by inversion symmetry, defined as  $\tau$  TLSs. CN rotations constitute asymmetric (S) TLSs. For two CN impurities in an otherwise pure lattice we find that the elastic S-S, S- $\tau$ , and  $\tau$ - $\tau$  interactions differ both in their magnitude at short distances, and in their spatial power law dependence. Introducing disorder does not change the relative magnitude of the interactions at short distances, but affects the spatial dependence of interactions involving a  $\tau$ -TLS, as inversion symmetry is broken. Our results are in agreement with theoretical predictions both for the magnitude and the power law dependence of the interactions. For the latter, we find that the power law dependence predicted for large distances persists down to very short distances, not much larger than the interatomic distance. Since the magnitude and spatial dependence of the elastic S- $\tau$  interactions is a crucial element in the Two-TLS model for the low temperature universality in disordered and amorphous solids, our results contribute to the validation of the above model, and to the advance of our understanding of the microscopic structure of amorphous solids and of the low temperature properties of glasses.

*Acknowledgments* — We thank A. Gaita-Ariño, Niels Grønbech-Jensen, and Joerg Rottler for very useful discussions. This research was supported by the Israel Science Foundation (Grant No. 982/10).

- 
- [1] P. W. Anderson, B. I. Halperin, and C. M. Varma, *Phil. Mag.* **25**, 1 (1972).
  - [2] W. A. Phillips, *J. Low Temp. Phys.* **7**, 351 (1972).
  - [3] R. C. Zeller and R. O. Pohl, *Phys. Rev. B* **4**, 2029 (1971).
  - [4] J. Jackle, *Z. Phys. B* **257**, 212 (1972).
  - [5] J. L. Black and B. I. Halperin, *Phys. Rev. B* **16**, 2879 (1977).
  - [6] M. Schechter and P. C. E. Stamp, *J. Phys.: Condens. Matter* **20**, 244136 (2008).
  - [7] A. L. Burin, *J. Low Temp. Phys.* **100**, 309 (1995).
  - [8] S. Rogge, D. Natelson, and D. D. Osheroff, *Phys. Rev. Lett.* **76** 3136 (1996).
  - [9] S. Ludwig, P. Nalbach, D. Rosenberg, and D. D. Osheroff, *Phys. Rev. Lett.* **90** 105501 (2003).
  - [10] M. Schechter and P. C. E. Stamp, *arXiv:0910.1283*.
  - [11] S. Hunklinger and A. K. Raychaudhuri, *Prog. Low Temp. Phys.* **9**, 265 (1986).
  - [12] R. O. Pohl, X. Liu, and E. Thompson, *Rev. Mod. Phys.* **74**, 991 (2002).
  - [13] J. P. Sethna and K. S. Chow, *Phase Trans.* **5**, 317 (1985).
  - [14] M. P. Solf and M. W. Klein, *Phys. Rev. B* **49**, 12703 (1994).
  - [15] A. Gaita-Ariño and M. Schechter, *Phys. Rev. Lett.* **107**, 105504 (2011).
  - [16] X. Liu, P. D. Vu, R. O. Pohl, F. Schiettekatte, and S. Roorda, *Phys. Rev. Lett.* **81**, 3171 (1998).
  - [17] R. O. Pohl, X. Liu, and R. S. Crandall, *Current Opin. Sol. St. Mat. Sci.* **4**, 281 (1999).
  - [18] A. Churkin *et. al.*, in preparation.
  - [19] J. F. Berret, P. Doussineau, A. Levelut, M. Meissner, and W. Schon, *Phys. Rev. Lett.* **55**, 2013 (1985).
  - [20] J. J. De Yoreo, W. Knaak, M. Meissner, and R. O. Pohl, *Phys. Rev. B* **34**, 8828, (1986).
  - [21] D. G. Bounds and M. L. Klein, *Mol. Phys.* **47(3)**, 629 (1982).
  - [22] M. L. Klein and I. R. McDonald, *J. Chem. Phys.* **79(5)**, 2333 (1983).